12th International Conference on CANDU Fuel
Holiday-Inn Waterfront Hotel
Kingston, Ontario, Canada, 2013 September 15-18

IRRADIATION BEHAVIOUR OF Th-Pu AND U-Pu MOX FUELS

Prerna Mishra, H.N. Singh, V.P. Jathar, R.S. Shriwastaw, P.M. Satheesh,
P.B. Kondejkar, G.K. Mallik, J.L. Singh and S. Anantharaman

Post Irradiation Examination Division,
Bhabha Atomic Research Centre,
Trombay, Mumbai-400085
E-mail: prernam@barc.gov.in

ABSTRACT - An experimental fuel pin cluster, comprising of twelve fuel pins of PHWR design and filled with fuel pellets of different chemical composition, was irradiated in the research reactor, CIRUS. The average burnup of the fuel cluster was 4.5 GWd/t(HM) and the peak burnup of the highest rated fuel pin of the cluster was 10.8 GWd/t(HM). After irradiation, the fuel pins of the cluster were subjected to detailed post-irradiation examination (PIE) to assess the performance of the fuel pins. The PIE included visual examination, dimension measurement, ultrasonic testing, gamma scanning, fission gas analysis and microstructural examination. No defect was observed on the cladding of the fuel pins. The fission gas release in the fuel pins was very low and no fuel restructuring was observed. This paper describes the post-irradiation examinations carried out and presents the results and conclusions.

Introduction

India has one of the world's largest deposits of thorium and relatively much smaller deposits of uranium. In view of the above, thorium utilisation is long term core objective of the Indian Nuclear Power Programme and thorium based fuels are to be used in the third stage of the programme [1, 2]. Unlike natural uranium which contains the fissile isotope, U^{235}, thorium does not contain any fissile isotope [3]. However, natural thorium can be converted to a fissile isotope U^{233} in a power/ breeder reactor. Fissile material like Pu^{239} in mixed oxide (MOX) fuels acts as a seed material and aids to convert natural thorium to fissile U^{233} [4].

Although the crystal structure of both, UO_2 and ThO_2 is CaF_2 type, there are certain differences in their properties [5]. Thoria is a stable oxide and has a very little non-stoichiometry as compared to UO_2. Thoria is chemically very stable and has a high melting point, low vapour pressure and higher thermal conductivity than urania.

PIE carried out on Thoria based MOX fuels have been reported to show good performance under irradiation [6, 7, 8]. In order to evaluate the irradiation behaviour of mixed thoria-plutonia and urania-plutonia fuel, an experimental fuel pin cluster comprising of twelve fuel pins of PHWR design with fuel pellets of different chemical compositions was irradiated in the Pressurized Water Loop (PWL) of CIRUS. The fuel pins in the cluster contained pellets of UO_2, ThO_2, $(Th\text{-}6.75\%Pu)O_2$ and $(U\text{-}3\%Pu)O_2$ encapsulated in collapsible, graphite coated Zircaloy-2 cladding. As a part of post irradiation examination, visual examination, dimension measurement, ultrasonic testing, gamma scanning, fuel pin puncturing and fission gas release measurement and microscopic examination using optical and scanning electron microscopy on the fuel pins of the fuel cluster have been carried out inside the hot-cells.

1. Fuel cluster design and fabrication details

PHWR-type fuel pins with fuel pellets of different chemical compositions were assembled in a two-tier cluster. The schematic of a typical fuel pin from BC-8 cluster is shown in Figure 1.

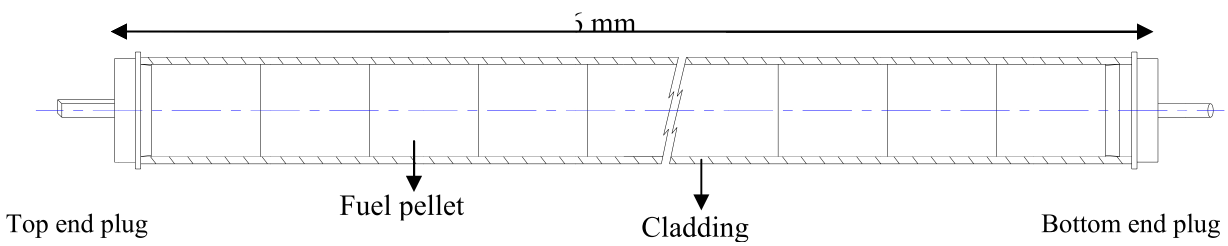

Figure 1 Schematic of a fuel pin of the BC-8 Cluster.

The tier-1 had 3 pairs of fuel pins, with one pair each of natural UO_2 pellets, $(U,Pu)O_2$ and $(Th,Pu)O_2$. The fuel pins were arranged in a circular geometry. Fuel pins of similar composition were placed on diametrically opposite ends of the cluster. Tier-2 consisted of six fuel pins containing ThO_2 pellets. The fuel pellets were encapsulated in graphite coated Zircaloy-2 clad with wall thickness of 0.38 mm. Helium was used as the filler gas in all the fuel pins. Table 1 provides the details of the fuel pins of the cluster.

Table 1 Description of the fuel pins in the BC-8 cluster

Pin identification		**P-01, P-02**	**M-01, M-02**	**U-01, U-02**
Pellet composition		$(Th\text{-}6.75\%Pu)O_2$	$(U\text{-}3\%Pu)O_2$	UO_2
PuO_2 enrichment, %		6.75	3	Nil
Pellet diameter, mm		14.3	14.2	14.3
Pellet length, mm		13.9	13.9	14.7
Pellet density, %		94.6	96.4	96.3
Cladding wall diameter, mm	outer	15.26	15.26	15.26
	inner	14.5	14.5	14.5
Grain size in the pellet, µm		Duplex microstructure with large grains (~28) & small grains (2-5)	Large grain size pellets`~40 and normal grain size pellets (4-12)	6-12

The fuel pellets were fabricated by powder metallurgy route involving cold compaction and high temperature sintering. The fuel pin designated as M-02 in the cluster consisted of $(U\text{-}3\%Pu)O_2$ pellets with large grain size (~40 µm) and a few pellets of normal grain size (4-12 µm). Large grain size pellets were fabricated by addition of 0.05 wt% TiO_2. ThO_2 and $(Th\text{-}Pu)O_2$ pellets contained 500 ppm of MgO, which was used as the sintering aid.

2. Irradiation history

The experimental fuel pin cluster was irradiated in the pressurised water loop (PWL) of CIRUS research reactor. The thermal neutron flux in the loop was 5×10^{13} n/cm^2/sec and the temperature and pressure of the light water coolant in the loop were 240^{o}C and 105 kg/cm^2 respectively. The peak linear heat rating of the fuel pins was 42 kW/m. The fuel cluster was irradiated up to a calculated average fuel burnup of 4.5 GWd/t(HM). The burnup of the peak rated fuel pin was calculated to be 10.8 GWd/t(HM).After irradiation and cooling for 13 years, the fuel pin cluster was transported to the hot cell facility for post irradiation examination.

3. Post Irradiation Examination

3.1 Visual examination

The fuel pins were dismantled from the cluster and visual examination was carried out on the individual pins using a wall mounted periscope. No abnormality or surface defect of any type was visible on of the cladding of the fuel pins. Figure 2 shows the periscopic view of the two tiers of fuel pins in the cluster.

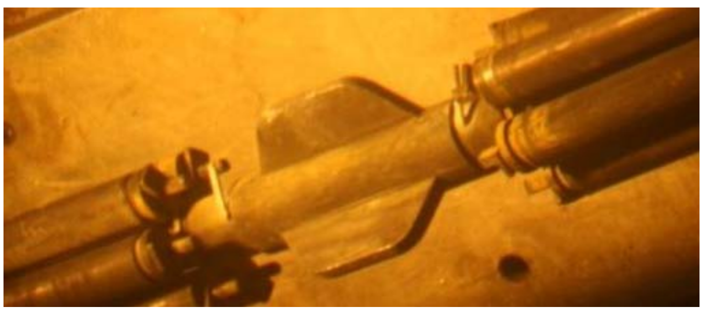

Figure 2 Periscopic view of the two tiers of fuel pins in the cluster

3.2 Fuel pin diameter measurement

The fuel pin diameters were measured using a remotely operated dial gauge. Average of three readings taken at three different orientations of the pin at each axial location was taken as the diameter at that location. Measurements were taken at an interval of 10 mm along the length of the fuel pin. The standard deviation in the diameter readings was 0.02. The measurements showed a reduction in the diameter of the fuel pins in all the 12 fuel pins compared to their as-fabricated diameter. The results of the diameter measurement carried out on the irradiated pins in comparison with the as-fabricated pins are plotted and shown in Figure 3. Maximum reduction in the diameter of ~0.2 mm was observed for (U-Pu)O_2 MOX and UO_2 pins. Minimum reduction in diameter of ~0.1 mm was observed in ThO_2 pins as shown in Figure 4.

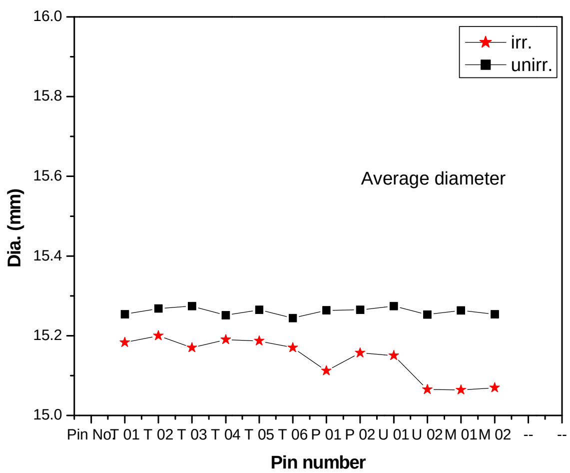

Figure 3 Average diameter of the fuel pins before and after irradiation

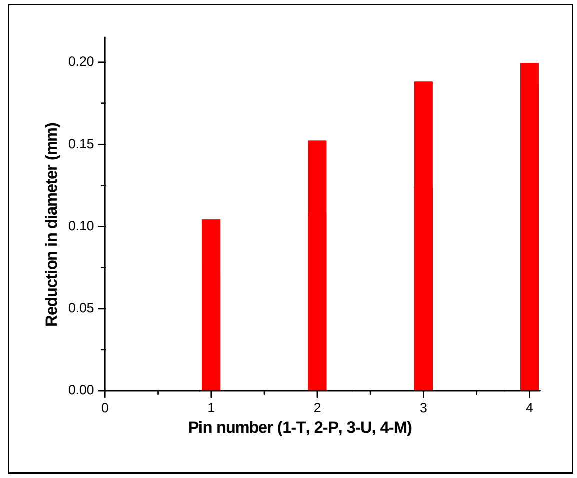

T- ThO_2 fuel pins, P- (Th-6.75%Pu)O_2 fuel pins, U- UO2 fuel pins, M- (U-3%Pu)O_2 fuel pins

Figure 4 Reduction in diameter observed in the fuel pins of the cluster

3.3 Ultrasonic testing

Two 10 MHz line focused ultrasonic transducers were used to detect the service induced defects in the clad. The transducers were inclined at 28^o to generate 45^o shear waves inside the cladding. Calibration notches of depth 10% of wall thickness were used to set the testing sensitivity. The two probes were fitted in a probe carriage immersed in water. Probes were translated to complete the scanning of fuel length. The fuel pin was rotated to achieve helical scanning. A marker was fitted to create an impression to identify the defect location after testing. The cladding of the fuel pins from the cluster was found to be free from any defects.

3.4 Gamma spectrometry and gamma scanning

A liquid nitrogen cooled HPGe detector and a PC based multichannel analyzer (MCA) were used for gamma spectroscopy and isotopic gamma scanning. The gamma-ray spectrum obtained from the spent fuel showed intense gamma ray peaks of Cs^{137}, Cs^{134} and Co^{60} in most of the fuel pins. The spectrum obtained from a (U-3%Pu)O_2 fuel pin is shown in Figure 5a. The presence of 2.6 MeV energy from Tl^{208} was noticed in ThO_2 and (Th-6.75%Pu)O_2 fuel pins as shown in Figure 5b.

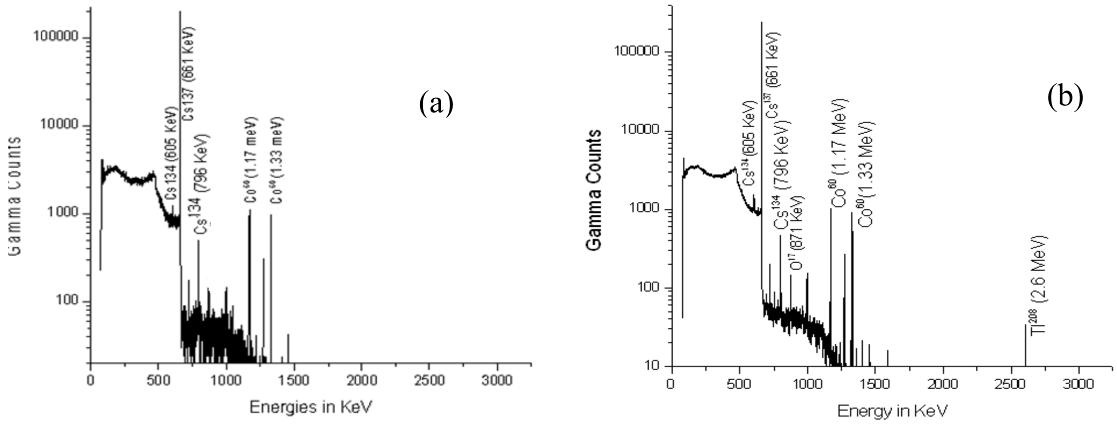

Figure 5 Gamma spectrum of (a) (U-3%Pu)O_2 fuel and (b) (Th-6.75% Pu)O_2 fuel

Significant variation in the Cs^{137} activity was observed in the MOX fuel pins as a function of axial position in the reactor (Figure 6a and 6b). The Cs^{137} counts of these fuel pins were found to increase towards the reactor centre and follow the flux profile in the reactor.

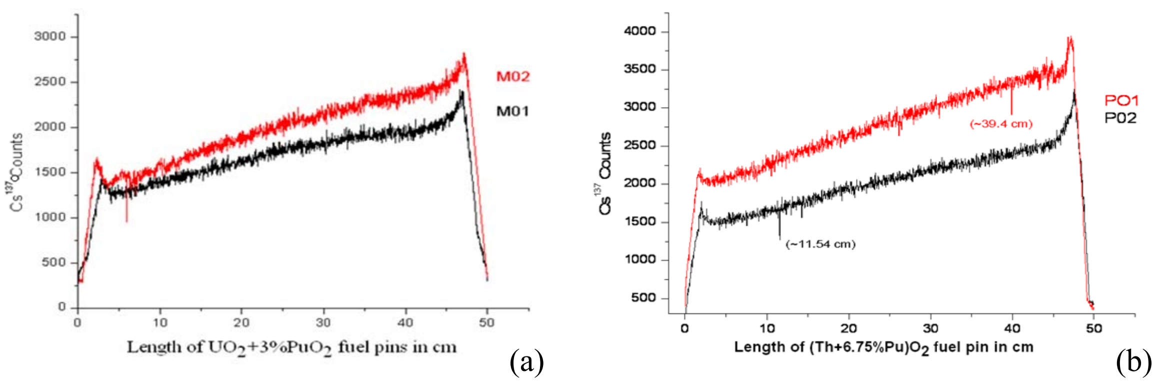

Figure 6 Axial gamma scanning of (a) (U-3%Pu)O_2 fuel pins and (b) (Th-6.75% Pu)O_2 fuel pins

The results of gamma scanning, carried out on all the fuel pins representing the relative counts of Cs^{137} along its length, are shown in Figure 7. Figure 8 shows the relative Cs^{137} activity of all the fuel pins.

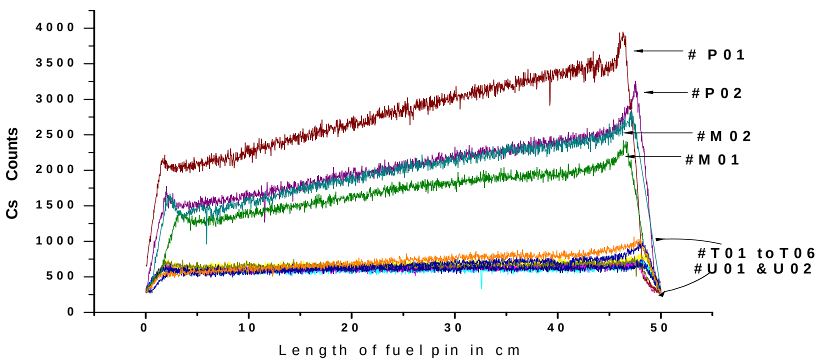

Figure 7 Gamma scanning of all the fuel pins of the cluster

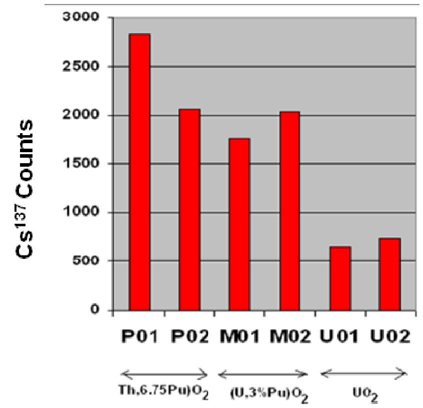

Figure 8 Relative Cs^{137} activity of all fuel pins

3.5 Fission gas analysis

Measurements of released fission gases on the irradiated fuel pins were carried out by puncturing individual pins under vacuum and collecting the gases. The chemical composition of the released gases was measured using a gas chromatograph. Void volume inside the fuel pin was measured to arrive at the internal pressure of the fuel pins. The results of fission gas release measurement in the six fuel pins are given in the Table 2. The values of the burn up of the fuel pins given in the table was estimated using the values of the average burnup of the fuel cluster, the peak burn up of the highest rated fuel pin and the relative gross gamma activity of the fuel pins. The results show very low fission gas release in the fuel pins.

Table-2: Results of fission gas release measurements

Pin Nos.	Fuel Composition	Burnup (GWd/t)	Fission Gas Generated (cc)	Internal pressure (atm)	Volume of fission gases at STP (cc)	% FGR
M-01	(U-3%Pu) O_2	6.9	150	1.33	0.07	0.05
M-02	(U-3%Pu) O_2	8.0	182	1.59	0.03	0.02
P-01	(Th-6.75% Pu) O_2	10.8	217	2.87	0.75	0.35
P-02	(Th-6.75% Pu) O_2	8.1	163	1.52	0.87	0.54
U-01	UO_2	2.5	58	1.99	0.02	0.03
U-02	UO_2	2.9	67	1.40	0.02	0.03

3.6 Ceramography/ metallography

3.6.1 Fuel microstructure

Metallographic examination has been carried out on the samples taken from (Th-Pu)O_2 MOX, (U-Pu)O_2 MOX and UO_2 fuel pins and are designated as P-02, M-02 and U-02 respectively. Metallographic samples were prepared inside the hot cells and examined using a remotised metallograph. Figure 9 shows the photomicrographs of the fuel section taken from the three fuel pins. Macroscopic examination of the fuel sections of the fuel pin revealed fine radial cracks. White particles were observed in the fuel cross sections taken from the MOX fuel pins. These particles did not show β-γ activity nor α-activity. The porosity distribution observed in the fuels was comparable to that in the as-fabricated fuel.

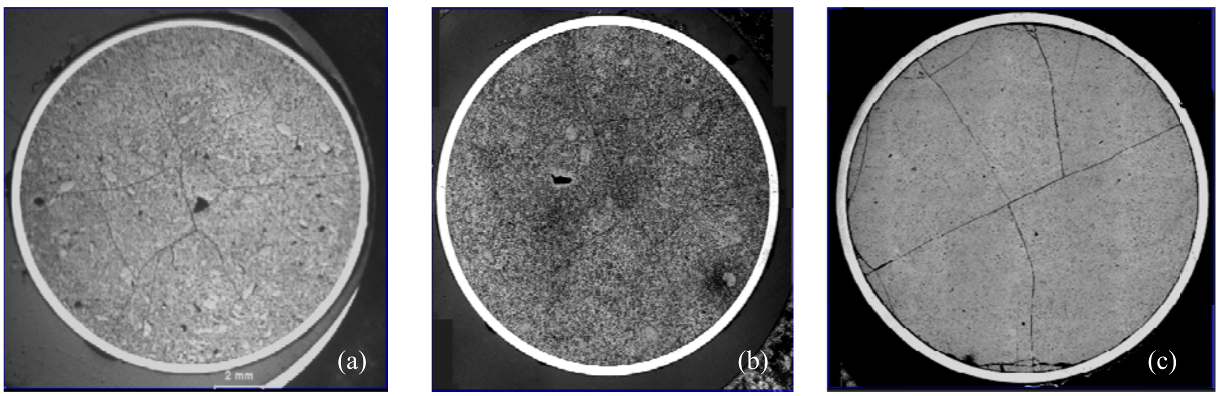

Figure 9 Photomacrographs of the fuel section from fuel pins (a) P-02, (b) M-02 and (c) U-02

Due to the chemical inertness of Thoria, conventional etching techniques to reveal the fuel microstructure were not suitable. Hence, replicas were prepared from the fractured pieces of the (Th-Pu)O_2 fuel from pin P-02 and the replicating foil having the impression of the grains (Figure 10a) were examined under a scanning electron microscope (SEM). The average grain size in the fuel was observed to be 30 µm.

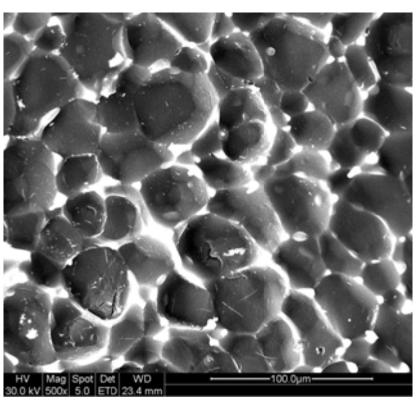

Figure 10 (a) Replica of fractured piece of (Th-Pu)O_2 fuel

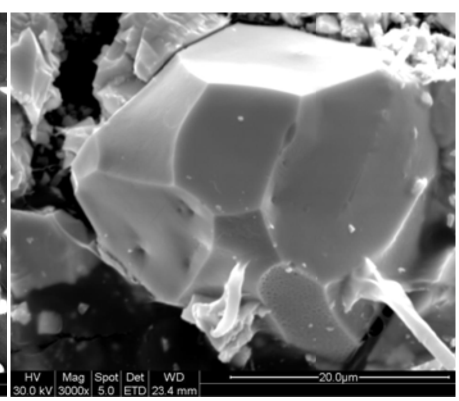

Figure 10 (b) Single grain of (Th-Pu)O_2 fuel

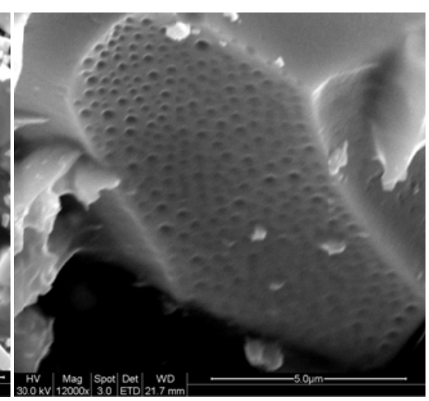

Figure 10 (c) fission gas bubbles on the grain face

A few grains of the fuel got transferred to the replicating foil and one such grains is shown in Figure 10b. Fission gas bubbles were noticed on one of the faces of the grain and the magnified view of the grain face is shown in Figure 10c. Presence of fission gas bubbles on a face of the grain of $(Th\text{-}Pu)O_2$ fuel and other faces devoid of the bubbles denotes the presence of a plutonium rich region at that face. High concentrations of plutonium termed as high fission areas in $(U\text{-}Pu)O_2$ fuel were also observed by Harrison etal [9].

Examination of the section taken from the large grain size pellet of the $(U\text{-}Pu)O_2$ fuel pin, M-02 revealed pores with bright and dark patches in the fuel cross section (Figure 11a). At higher magnification, larger grains with an average size of 30 μm were observed in the bright regions of the fuel and fine grains of the size 5 μm with fine pores in the dark regions. Larger grains are observed in the vicinity of big pores as shown in Figure 11b. Rounded type big pores were observed in the fuel and the average size of the pore was ~16 μm. Figure 11c shows the fine grains and pores observed in the fuel. The grain size observed in the fuel was similar to that in the as-fabricated fuel, indicating no grain growth during irradiation.

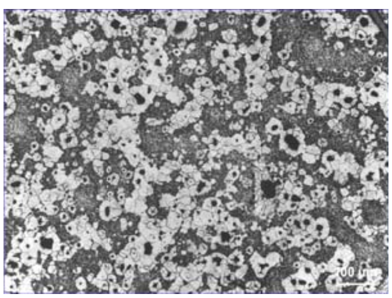

Figure 11 (a) Bright and dark regions in the $(U\text{-}Pu)O_2$ fuel

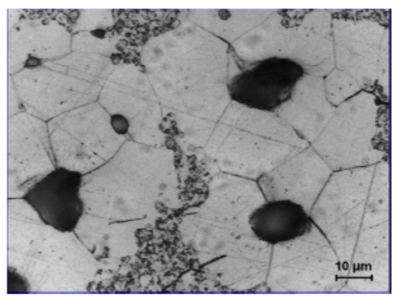

Figure 11 (b) Pores and large grains in $(U\text{-}Pu)O_2$ fuel

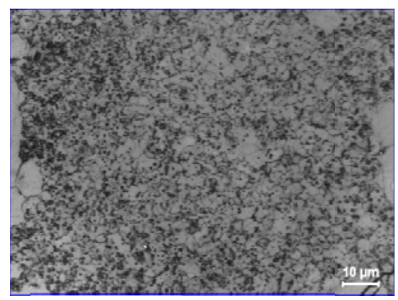

Figure 11 (c) Fine grains and pores in $(U\text{-}Pu)O_2$ fuel

The UO_2 fuel examined from pin U-02 revealed equiaxed grains with an average grain size 12 μm at the center of the fuel. This was similar to the average grain size of 11 μm observed at the fuel periphery and that in the as-fabricated fuel. This indicates that there was no grain growth in the fuel.

3.6.2 <u>Clad corrosion and hydriding</u>

Continuous oxide layer was observed on the outer surface of the clad of all the fuel pins of the cluster with an average oxide layer thickness in the range of 1.6 μm to 2.5 μm. Variation in the thickness of the oxide layer was observed on the inner surface of the clad in the fuel pins of the cluster. Oxide layer could be seen at a very few locations with the average thickness 1.2 μm in P-02 whereas a continuous layer was observed in the cladding of fuel pins M-02 and U-02 with the average thickness being 3.3 and 28 μm (Figure 12 a, b and c).

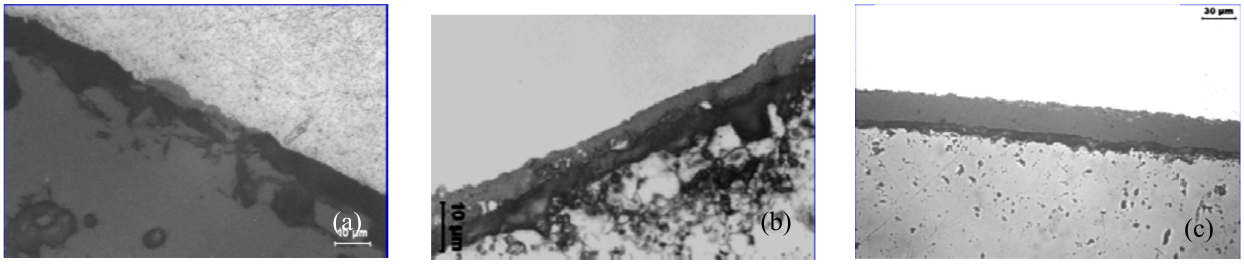

Figure 12 Oxide layer on the inner surface of the cladding of fuel pin (a) P-02 (b) M-02 (c) U-02

The extent of hydriding in the cladding of the fuel pins M-02 and U-02 was examined. The hydride platelets in the cladding taken from both the pins were circumferentially orientated but the size and density of the platelets was more in the cladding from U-02 fuel pin, indicating higher hydrogen pick up in the cladding due to higher oxidation on the inner surface of the cladding.

4. Summary and conclusions

Post irradiation examination of $(Th\text{-}6.75\%Pu)O_2$ fuel pins, $(U\text{-}3\%Pu)O_2$ MOX fuel pins and UO_2 fuel pins of BC-8 cluster irradiated in pressurized water loop of CIRUS up to an average fuel burnup of 4.5 GWd/t has been carried out to assess the irradiation performance of the fuel. The main findings are presented below.

1. All the pins were found to be intact after irradiation without any abnormal corrosion.

2. Reduction in the diameter of the fuel pins was observed as compared with their as-fabricated diameter. This is attributed to the creep collapse of the cladding. The maximum clad collapse was observed for $(U\text{-}Pu)O_2$ MOX and UO_2 pins, minimum collapse was observed in ThO_2 pins.

3. The gamma-ray spectrum obtained from the spent fuel showed intensive gamma ray peaks of Cs^{137} (661 keV) , Cs^{134} (604 and 796 keV) and Co^{60} (1170 and 1330 keV) in all the types of fuel pins. Co^{60} is an activation product present in the clad of the fuel pin. The presence of 2.6 MeV energy from Tl^{208} was observed mainly in ThO_2 and $(Th\text{-}6.75\%Pu)O_2$ fuel pins and is expected from the daughter products of U^{232}.

4. The fission gas release in the fuel pins is very low.

5. Restructuring of the fuel was absent in all the fuel pins. This indicates that the fuel centre temperature was not high enough for restructuring or fission gas release.

6. Thickness of the oxide layer on the outer surface of the cladding due to water side corrosion was similar in the three pins. However there was a large variation in the oxide layer (due to fuel-clad interaction) thickness on the inner surface of the cladding. Higher cladding

corrosion and hydriding observed in the UO_2 fuel pin is believed to be due to the presence of higher content of moisture in the fuel pellets.

5. Acknowledgements

The authors are thankful to Shri D. N. Sah for useful suggestions provided in preparation of the manuscript. They would also like to express thanks the Shri Shailesh Katwankar, Shri S.R.Soni and other members of the hot cell facility for the assistance provided in the PIE of the fuel pins.

6. References

1. IAEA-TECDOC-1450, "Thorium Fuel Cycle- Potential benefits and challenges" May-2005.

2. "Atomic Energy in India: A Perspective" Government of India, Department of Atomic Energy, Sept 2003.

3. Michel Lung, Otto Gremm, Nuclear Engineering and Design 180 (1998) 133–146.

4. S. Sivasubramanian, S.M. Lee, S.A. Bharadwaj, "Current status and future possibilities of thorium utilisation in PHWRs and FBRs", Proceedings of the Annual conference of Indian Nuclear Society (INSAC-2000)IT-1, Page 16.

5. J. Belle, R.M. Berman, "Thorium Dioxide- Properties and Nuclear Applications", Technical Report DOE/NE-0060, 1984 Jan 01.

6. G. Horhoianu, G. Olteanu, D.V. Ionescu, "Irradiation behaviour of PHWR Type Fuel elements Containing UO_2 and (Th, U)O_2 Pellets", IAEA technical meeting on "Fuel integrity during normal operation and accident conditions in pressurized heavy water reactors (PHWRs)", Romania, Bucharest, September 24–27, 2012.

7. M. Karam, F.C. Dimayuga and J. Montin, "Post-Irradiation Examination of CANDU fuel bundles fuelled with (Th, Pu)O_2", Proceedings of the 11th Int. Conf. on CANDU Fuel, Niagara Falls, Ontario, (2012).

8. P.G. Boczar, P.S.W. Chan, G.R. Dyck, R.T. Jones, J.D. Sullivan, and P. Taylor, "Thorium Fuel-Cycle Studies for CANDU Reactors", IAEA Meeting on "Thorium Fuel Utilization: Options and Trends", IAEA-TECDOC-1319 (2002 November).

9. N.F.Harrison, T. Janathasing, F.C. Dimayuga, "Post-Irradiation Examination of MOX fuel with varying plutonium homogeneity", Proceedings of the 11th Int. Conf. on CANDU Fuel, Niagara Falls, Ontario, (2012).